

**OPEN ACCESS**

## Laser beam optical CT scanner for in-air gel readout: imaging artefacts

To cite this article: D Ramm 2013 *J. Phys.: Conf. Ser.* **444** 012078

View the [article online](#) for updates and enhancements.

### You may also like

- [A model of p-branes with closed-constraint algebra](#)  
M N Stoilov and D T Stoyanov
- [Ion implantation in semiconductors](#)  
G Dearnaley, K Kandiah and R S Nelson
- [A hierarchy of lattice soliton equations and its Darboux transformation](#)  
Ding Hai-Yong, Xu Xi-Xiang and Zhao Xiang-Dong

**ECS**  
The  
Electrochemical  
Society  
Advancing solid state &  
electrochemical science & technology

**DISCOVER**  
how sustainability  
intersects with  
electrochemistry & solid  
state science research

# Laser beam optical CT scanner for in-air gel readout: imaging artefacts

**D Ramm**

Department of Medical Physics, Royal Adelaide Hospital Cancer Centre, South Australia, Australia  
School of Chemistry and Physics, University of Adelaide, South Australia, Australia

E-mail: daniel.ramm@health.sa.gov.au

**Abstract.** Ongoing progress on development of an in-air scanning optical CT is reported, specifically dealing with the minimization of scanner imaging artefacts. Improved scratch resistance of the PMMA gel cylinder was a primary goal, so that routine cleaning would not degrade the polished surfaces. This was achieved by the addition of a hard coating to the cylinder surfaces. New artefacts were introduced and subsequently reduced by alternative processing of projection data. The outcome was a gel cylinder of much greater practicality for routine use while maintaining similar signal to noise ratios and uniformity in the image reconstruction field of view.

## 1. Introduction

Optical CT scanning of dosimetric gels [1] usually requires the use of a RI matching fluid bath to reduce refraction and reflection effects at the surface of the cylindrical gel container. Recently we have developed an 'in-air scanner' that avoids the use of a fluid bath while obtaining effectively parallel ray projection data for 90 % of the gel sample diameter [2]. Previously Maryanski and Ranade developed the 'dry scanner' intended mainly for brachytherapy source applications [3]. This scanner cannot accurately image optical attenuation outside a small central region of the gel dosimeter since it only acquires projection data for about 36 % of the gel diameter. Another approach using the PRESAGE [4] dosimeter has been proposed, using algebraic reconstruction to account for non-parallel light rays [5]. Limited projection data (65 % of PRESAGE diameter) was still a limiting issue for that simulation study. Our in-air scanning approach is the only one realized to demonstrate the feasibility of scanning external beam irradiated gels without RI matching fluid.

While the principle of the prototype in-air scanner's operation has been shown, further developments are required in preparation for radiotherapy clinical application. One aspect is imaging artefacts [6, 7] that degrade 3D dosimetric data and can present a significant obstacle in gaining high quality measured data and general acceptance of the dosimetry method. Preliminary results indicated some readily observable artefacts [2]. These artefacts have been under investigation, together with some others that have become apparent.



## 2. Methods

### 2.1. Optical CT scanner

The scanner is detailed in [2], with brief summary as follows. A He-Ne laser beam is fanned by a rotating mirror across the key component, a machined and polished PMMA cylinder (76 mm outer diameter (OD), 51 mm inner diameter (ID)). Inside the cylinder is the gel, and after the laser beam passes through with close to parallel ray geometry, it is refracted by the cylinder walls to a focal point at a silicon photodiode detector. With the ID/OD ratio of around 67 % and FXG inside, parallel rays extend to about 90 % of the gel diameter. Extrapolation of the missing projection ends is applied prior to back-projection.

Changes to the original scanner details include the following: (i) A revised bearing assembly for the sample rotation mechanism, giving improved rotational precision. (ii) The PMMA cylinder internal and external walls were hard coated with a scratch resistant coating (Crystalcoat MP-101, SDC Technologies). This polysiloxane based coating had a measured thickness of  $3.8 \pm 0.1 \mu\text{m}$  over the cylinder surfaces. (iii) Improved gel optical quality by using a syringe with filter (2  $\mu\text{m}$  nominal pore size) to fill the gel containers. (iv) An option for low pass filtering of projection data and re-sampling to 0.4 mm. (v) An option for point by point division of measurement projection data by reference scan data for the entire cylinder, as opposed to the original method of a single averaged reference scan projection for normalization.

### 2.2. Imaging artefacts

The three most apparent artefacts identified previously were: (i) An outer ring in the extrapolation region due, in part, to mechanical imprecision of the sample rotation. (ii) Small spots in the sample due to foreign particles (dust). (iii) Low level streaking due to scratches or dust on the cylinder walls. Additionally, cylinder wall scratching through routine cleaning was a chief concern because severe streak artefacts can result. Attempts to improve these artefacts have been made by the aforementioned changes to the scanner.

Another potential source of artefacts is inter-reflection, ie. multiple reflections between optical components. One instance was reflected light from the photodiode surface back-reflected to itself by the cylinder. This was previously addressed by tilting the photodiode so that the reflection was not incident upon the cylinder. There is a more subtle effect where the beam is reflected from the exit wall of the cylinder (PMMA-air interface) back to the entry wall, and then towards the photodiode. Since air-PMMA interface reflectance is about 4 % in the worst case (for the acquired range of data) this signal can only amount to 0.2 %, and less with gel attenuation.

Optical interference effects are particularly important to avoid because signal modulation of several percent may be introduced. This has been observed at the central axis of the cylinder where cylinder inter-reflections can, at times, result in constructive and destructive interference. A significant transient waveform in the centre of projection data can occur, particularly when there is minimal attenuation in the cylinder. Interference effects can also be introduced where coatings are applied to components, such as the hard coating on the PMMA cylinder. With the current hard coating there is a mismatch in RI ( $n_{\text{coating}} = 1.45$ ,  $n_{\text{PMMA}} = 1.49$ ), leading to a change in transmission at an air-coating-PMMA interface of about 0.5 % for a 0.1  $\mu\text{m}$  (typical) change in coating thickness ( $\lambda = 594 \text{ nm}$ ).

To investigate and illustrate the artefacts, the cylinder was filled with filtered distilled water and green dye water solutions. Undyed scans were used as the reference scan throughout, and an undyed measurement scan was used to examine low level effects (mainly interference). These effects are more evident in this case than scans with significant optical attenuation in the cylinder. Scans of water samples with uniform attenuation were made with dye solutions of moderate ( $\text{OD}_{\text{moderate}} = 0.18 \text{ cm}^{-1}$ ) and high ( $\text{OD}_{\text{high}} = 0.50 \text{ cm}^{-1}$ ) levels. Reconstructed dose images were viewed and analyzed using ImageJ (National Institutes of Health, USA).

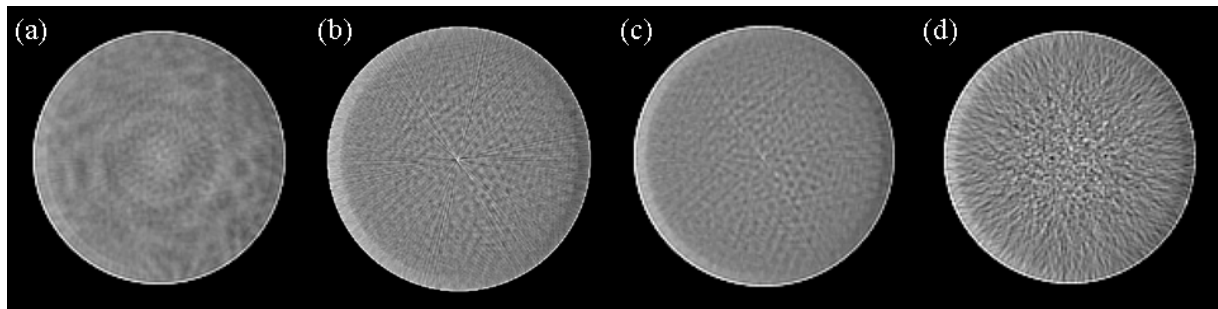


**Figure 1:** Reconstructed images of one slice for the green dye water filled cylinder, with viewing window widths of 20 % of the mean and centred on the mean value. (a)  $OD_{\text{moderate}}$ , 0.4 mm pixel size and averaged normalizing reference projection. (b)  $OD_{\text{moderate}}$ , 0.2 mm pixel and point by point reference scan normalization. (c) Same as 1(b) except for projection filtering and 0.4 mm pixel. (d) Same as 1(c) except for  $OD_{\text{high}}$ .

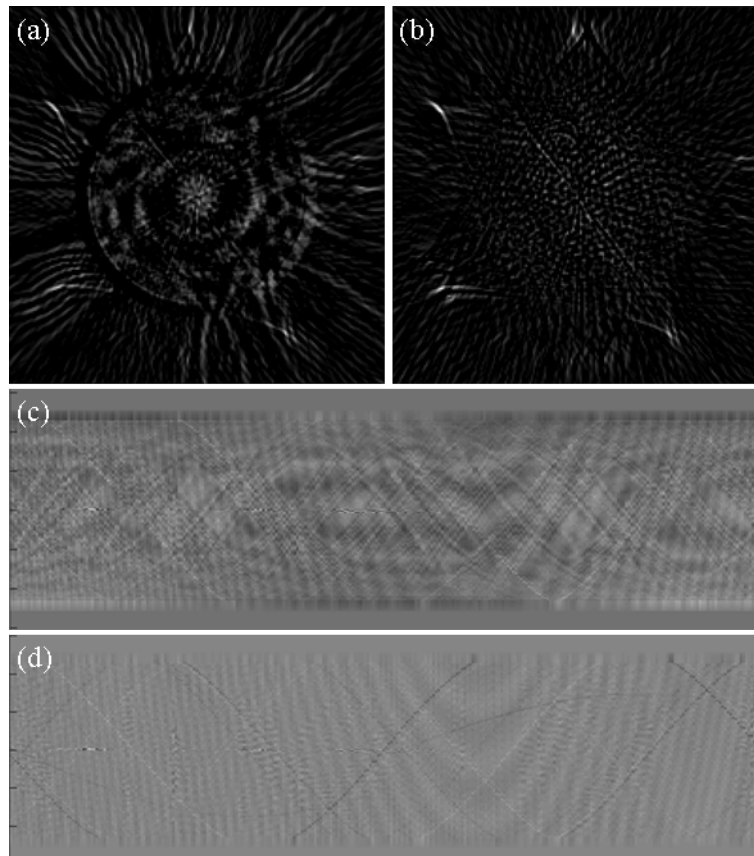


**Figure 2:** Undyed water scan normalized to another undyed water scan, where the ideal result would be a blank image. (a) Reconstructed slice using an averaged reference projection. Viewing window width 5 % of mean pixel value for  $OD_{\text{moderate}}$ . Interference artefacts appear inside and outside the internal volume of the cylinder. (b) Same as 2(a) except for point by point reference division, giving reduced interference artefacts. (c) Sinogram for 2(a) showing superimposed multiple interference patterns. (d) Sinogram for 2(b) with less interference patterns. The thin lines (dark from reference scan and light from measurement scan) are due to dust specks on the outer cylinder surface.

### 3. Results and discussion

A reconstructed slice of dyed water ( $OD_{\text{moderate}}$ ) is shown in figures 1(a), 1(b) and 1(c). The same projection data was used for these three images, just differing in data processing. The most obvious non-uniformity feature of figure 1(a) was the patterned appearance that was new to this version of the scanner. The reason for this was due to interference effects from the addition of the hard coating on

the cylinder. Figure 2 shows more detail of these interference patterns. Figures 2(a) and 2(b) are reconstructed slices of undyed water scans normalized to another undyed scan with averaged reference projection (2(a)) and point by point reference projections (2(b)). The sinograms are shown in figures 2(c) and 2(d) where optical interference patterns become more discernible, particularly figure 2(c). Figure 2(b) and the corresponding sinogram, figure 2(d), show that the point by point reference division largely removes the coating interference effects. Figures 1(b) and 1(c) confirm the minimization of this interference effect. The hard coating is substantially more durable than a PMMA surface, meaning the cylinder surfaces can be routinely cleaned with reduced scratching concerns.

Another optical interference effect was an interference signal on the central axis shown in the sinograms of figure 2(c) and 2(d). There is a broken line of signals of high and low relative intensities running down the central axis. These manifest in reconstructions as radial lines as shown in figure 1(b). Since these interference waveforms in the projection data are of high frequency, filtering assists in their minimization as shown by figure 1(c). This interference effect is dependent upon the degree of attenuation by the sample with the worst case occurring for undyed water as used here for all reference projection data. When gel is used, the presence of attenuation even in FXG pre-irradiation reference scans, means this effect is usually minimal.

Figure 1(d) is a high OD example with central axis OD of about 2.5 (0.3 % transmission). Noise in the projection data becomes more significant, hence a random noise appearance dominates the residual artefacts of figure 1(c). The residual artefacts mainly comprise a mottled appearance originally thought to be caused by multiple low level streaking, however further investigation is required to confirm the source(s). There is still a remaining artefact in the extrapolation region, however it is not considered reliable FOV in any case, and does not affect the full data FOV.

To put the fluctuations observed in the images of figure 1 into perspective, 1(a) had a standard deviation in the FOV of 0.8 % of the mean value, 1(b): 1.3 %, 1(c): 0.8 % and 1(d): 2.0 %.

#### 4. Conclusions

Optical interference has been found to be a source of artefacts in the process of continued development of an in-air optical CT scanner. The addition of a hard coating to the gel cylinder provided greater scratch resistance, reducing the likelihood of streak artefact inducing scratches. However interference artefacts were also introduced. Point-by-point reference scan division helped minimize these effects. RI matched hard coating is planned for the future. A remaining structured mottle artefact in the FOV requires further investigation, however presently a signal to noise ratio of around 130 is obtained for a uniform moderate optical density.

#### 5. Acknowledgements

Application of the cylinder hard coating by Colin Hall, University of South Australia, and support by John Schneider, Royal Adelaide Hospital, Medical Physics workshop is gratefully acknowledged.

#### 5. References

- [1] Baldock C *et al* 2010 *Phys. Med. Biol.* **55** R1-63
- [2] Ramm D *et al* 2012 *Phys. Med. Biol.* **57** 3853-68
- [3] Maryanski M J and Ranade M K 2001 *Proc. of SPIE Int. Soc. Optic. Eng.* **4320** 764-767
- [4] Gorjiara T *et al* 2011 *Med. Phys.* **38** 2265-74
- [5] Doran S J and Yatigamma D N 2012 *Phys. Med. Biol.* **57** 665-83
- [6] Bosi S *et al* 2007 *Phys. Med. Biol.* **52** 2893-2903
- [7] Bosi S G *et al* 2009 *Phys. Med. Biol.* **54** 275-83